·Basic Research·

Age–related maculopathy susceptibility 2 participates in the phagocytosis functions of the retinal pigment epithelium

Yi-Ting Xu [1,2], Ye Wang [2], Peng Chen [2], Hai-Feng Xu [2]

[1]School of Medicine and Life Sciences of Shandong Academy of Medical Sciences, University of Jinan, Jinan 250022, Shandong Province, China

[2]State Key Laboratory Cultivation Base, Shandong Provincial Key Laboratory of Ophthalmology, Shandong Eye Institute, Shandong Academy of Medical Sciences, Qingdao 266071, Shandong Province, China

Correspondence to: Hai-Feng Xu. State Key Laboratory Cultivation Base, Shandong Provincial Key Laboratory of Ophthalmology, Shandong Eye Institute, Shandong Academy of Medical Sciences, Qingdao 266071, Shandong Province, China. chxhf@126.com

Abstract

• AIM: Age-related macular degeneration (AMD) is a multifactorial disease and a prevalent cause of visual impairment in developed countries. Many studies suggest that age-related maculopathy susceptibility 2 (ARMS2) is a second major susceptibility gene for AMD. At present, there is no functional information on this gene. Therefore, the purpose of the present study was to detect the expression of ARMS2 in retinal pigment epithelium (RPE) cells and to investigate the effect of ARMS2 on the phagocytosis function of RPE cells.

• METHODS: Immunofluorescence and reverse transcriptase PCR were used to demonstrate the presence and location of ARMS2 in ARPE-19 (human retinal pigment epithelial cell line, ATCC, catalog No.CRL-2302) cells. siRNA was used to knock down ARMS2 mRNA, and the effects of the knockdown on the phagocytosis function of the ARPE-19 cells were evaluated via Fluorescence Activated Cell Sorting (FACS).

• RESULTS: ARMS2 was present in ARPE-19 cells, localized in the cytosol of the perinuclear region. The expression of ARMS2 mRNA (messenger RNA) in ARPE-19 cells transfected with ARMS2-siRNA (small interfering RNA, 0.73± 0.08) was decreased compared with normal cells (1.00± 0.00) or with cells transfected with scrambled siRNA (0.95± 0.13) ($P<$ 0.05). After incubation of RPE cells with a latex beads medium for 12, 18, or 24 hours, the fluorescence intensities were 38.04 ± 1.02, 68.92 ± 0.92, and 78.00 ± 0.12 in the ARMS2-siRNA-transfected groups, respectively, and 77.98 ± 5.43, 94.87 ± 0.60, and 98.30 ± 0.11 in the scrambled siRNA-transfected groups, respectively. The fluorescent intensities of the same time points in the two groups were compared using Student's t-test, and the p values were all less than 0.001 at the three different time points.

• CONCLUSION: There is endogenous expression of ARMS2 in ARPE-19 cells. ARMS2 plays a role in the phagocytosis function of RPE cells, and this role may be one of the mechanisms that participates in the development of AMD.

• KEYWORDS: age-related maculopathy susceptibility 2; age-related macular degeneration; retinal pigment epithelium; phagocytosis

INTRODUCTION

Age-related macular degeneration (AMD), a progressive degeneration of the macula of the retina, is the leading cause of irreversible vision loss in older adults in developed countries [1]. Demographic changes with increasing life expectancy will lead to further increases in the number of affected individuals throughout the world. AMD has become a significant public health concern and a major focus of research efforts. AMD is likely a multifactorial disease resulting from interactions between genetic variants and environmental factors [2]. However, its precise etiology remains elusive. Recent studies have established the importance of genetic variations in the development of AMD [3,4]. A number of AMD-associated genetic variants have been reported, including the Y402H variant in the complement factor H (CFH) gene[5] and the A69S variant in the age-related maculopathy susceptibility 2 (ARMS2) gene[6]. The complement factor H (CFH) gene at 1q32 [5,7] was the first major gene to be associated with AMD. Weeks *et al* [8] identified the second major AMD susceptibility locus,

10q26, and it was further confirmed in some individual studies [9,10]. This evidence was also validated by a meta-analysis of several published reports, which provided the strongest evidence for an AMD susceptibility locus at 10q26 [11]. Three genes identified at 10q26 and associated with the risk of AMD are PLEKHA1 (Pleckstrin homology domain-containing protein family A member 1), ARMS2 (LOC387715/age-related maculopathy susceptibility 2), and HTRA1 (high-temperature requirement A1) [6,11,12]. Jakobsdottir *et al* [12] indicated an association of the SNPs overlying these genes but could not implicate any specific genes, while other studies have strongly suggested that an A69S single-nucleotide polymorphism (rs10490924) in exon 1 of the ARMS2 gene was the most likely susceptibility allele of AMD [6,13]. One study showed that after controlling for demographic and behavioral risk factors, heterozygosity for ARMS2 (A69A/A69S) is associated with an odds ratio (OR) of 1.69–3.0 for advanced AMD, while homozygosity for the risk-conferring allele (A69S/A69S) results in an OR of 2.20-12.1 [14]. A meta-analysis [15] suggested that, for the ARMS2 rs10490924 G→T polymorphism, TT homozygotes carry a 7.5-fold increased risk of AMD, while TG heterozygotes carry just a 2.4-fold increased risk of AMD, when compared with GG homozygotes.

In addition to the A69S variant, a deletion-insertion (indel) polymorphism variant in the 3'UTR of ARMS2 has also been significantly associated with AMD risk [16,17]. It was hypothesized that this variation causes a decrease in transcript stability, and homozygotes for the variant would lack ARMS2 protein expression, which could be due to unstable mRNA. Thus, the indel variant would affect mitochondrial homeostasis[16].However,Wang *et al*[18]. showed that the indel variant did not destabilize the transcript in human cell lines and suggested that the association with AMD might be due to the high linkage disequilibrium between the indel and A69S. Because the A69S and indel are in high linkage disequilibrium and occur on the same haplotype, the effects are not independent of each other.

Although CFH has been demonstrated as the first major AMD susceptibility gene, and ARMS2 was the second major susceptibility gene for AMD in Caucasian populations [6], in the northern Chinese population, the Y402H variant in CFH has not been associated with exudative AMD [19]. Other research groups in Hong Kong [20] and Japan [21,22] also reported that the Y402H variant was not associated with AMD, and this disparity may be due to ethnic differences. Contrary to the CFH Y402H variant, A69S (rs10490924) in ARMS2 has significant associations with exudative AMD and was the first risk allele identified in the Chinese population. The risk T-allele frequency of rs10490924 in ARMS2 was 64.9% in disease cases versus 43.2% in controls ($P<0.001$). The odds ratio for risk of AMD was 1.56 (95% CI; 0.80-3.03) for the GT genotype and 5.45 (95% CI; 2.59-11.49) for the TT genotype [19].

To date, an enormous number of studies have shown a significant association between ARMS2 and AMD, but the mechanism remains unknown. Thus, in the present study we investigated the biological function of ARMS2 by evaluating its effect on ARPE-19 phagocytosis. We found that phagocytosis was significantly decreased after ARMS2 suppression. Taken together, our results showed that ARMS2 is related to the RPE phagocytosis function and may subsequently participate in the pathogenesis of AMD.

MATERIALS AND METHODS

Materials

Cell culture ARPE-19 (human retinal pigment epithelial cell line, ATCC, catalog No.CRL-2302) cells were cultured in 1:1 of Dulbecco's modified Eagle medium/nutrient mixture F12 (DMEM/F12; Invitrogen, Carlsbad, CA, USA), containing 10% fetal bovine serum(FBS, Invitrogen),100 IU/mL penicillin G (Invitrogen), and 100μg/mL streptomycin (Invitrogen). The cells were incubated at 37℃ in a humidified atmosphere of 5% CO_2 and 95% air. The culture medium was changed every 3 days. After 90% confluence was reached, the cells were routinely passaged by dissociation in 0.05% trypsin/0.02% EDTA, followed by re-plating at a split ratio ranging from 1:2 to 1:4. For experiments, the cells were seeded in 96-, 48-, or 6-well plates, according to the different requirements.

Methods

Reverse transcriptase PCR Total RNA was extracted with a NucleoSpin RNAII Assay Kit (Macherey-Nagel, Düren, Germany) from ARPE-19 cells, according to the manufacturer's instructions. The first strand cDNA (complementary DNA) was synthesized from 1μg of total RNA in a 20-μL reaction mixture using a PrimeScript 1st Strand cDNA Synthesis Kit (TaKaRa, Dalian, China). One microliter of cDNA was then used for RT-PCR. PCR reactions were performed using GoTaq Flexi DNA polymerase (Promega, Madison, WI, USA) in a 10μL mixture containing 2μL 5×Colorless GoTaq Flexi Buffer, 2.5mmol/L $MgCl_2$, 0.25μmmol/L each of dNTP (Deoxyribonucleoside5'-Triphosphates), 0.25mol/L of each primer, 4 units GoTaq DNA polymerase, and 25ng cDNA. After an initial denaturation step at 95℃ for 3 minutes, amplification was performed for a total of 30 cycles under the following conditions: denature at 95℃ for 30 seconds, annealing at 40.7℃ for 30 seconds, and extension at 72℃ for 30 seconds. Then the final step was 72℃ for 10 minutes. A negative control substitution of water for the cDNA template was included in all experiments. The housekeeping gene β-actin was used as an internal control because it is believed to be continuously expressed at constant amounts in cells. PCR products were run on 2% agarose gel and

were visualized after ethidium bromide staining. The intensity of the bands was analyzed using NIH Image 1.62 software (National Institutes of Health, Bethesda, MD, USA). The primer sequences used for ARMS2 were forward-5'-TCG GTG GTT CCT GTG TCC TTC ATT-3', reverse-5'-TCA CCT TGC TGC AGT GTG GAT GAT-3' and for β-actin were forward-5'-ACC AAC TGG GAC GAC ATG GAG AAA-3', reverse-5'-ACT CCT GCT TGC TGA TCC ACA TCT-3'.

Immunocytochemistry ARPE-19 cells were seeded in 96-well plates. After different treatments, the cells were washed 3 times with PBS (phosphate-buffer saline) and then fixed in 4% paraformaldehyde for 10 minutes at room temperature and blocked with normal nonimmune goat serum (MAXIN BIO, Fuzhou, China) for 30 minutes at 37℃. The cells were then incubated overnight at 4℃ with rabbit polyclonal to ARMS2 (Abcam, Cambridge, UK) primary antibody. This step was followed by three washes with PBS and incubation for 1 hour with TRITC-conjugated goat anti-rabbit IgG (ZSGB-BIO, Beijing, China) at 37℃. After further PBS washes, the cell nuclei were stained with DAPI (4', 6-diamidino-2-phenylindole, Santa Cruz, Santa Cruz, CA, USA). Negative controls were stained by omitting the primary antibody. Images were captured using a laser confocal microscope (Nikon/C1 Plus; Nikon, Tokyo, Japan).

siRNA transfection The transfection reagent (FlexTube siRNA Premix) was purchased from QIAGEN (Hilden, Germany), including a siRNA designed for the human ARMS2 gene (cat. no. SI00507990, target sequence CTCCATGATCCCAGCTGCTAA) and a control siRNA, which contains a scrambled sequence (cat. no. SI03650318). FlexTube siRNA Premix was resuspended before first use, according to the manufacturer's protocol. The cells were seeded into 6-well plates one day prior to transfection. At the time of transfection with siRNA, the cells were approximately 60% confluent in 2mL of complete DMEM/F12 medium and then were transfected for roughly 24 hours with 42μL of transfection reagent diluted in 2mL of DMEM/F12 (HyClone, Thermo Fisher Scientific, Beijing, China) medium. The final concentrations of the siRNAs were 25nmol/L each. After transfection, the supernatant was removed from all wells, and some of the cells were incubated with complete DMEM/F12 medium for another 24 hours to monitor changes in ARMS2 expression with PCR or immunofluorescence, while the remaining cells were subjected to phagocytosis experiments.

Incubation of ARPE-19 cells with latex beads and quantification of phagocytosis Fluorescent latex beads (LBs, yellow-green, 1.0μm in diameter; SIGMA) were used to measure phagocytosis. Before being added to the wells, the beads were diluted in complete DMEM/F12 medium to
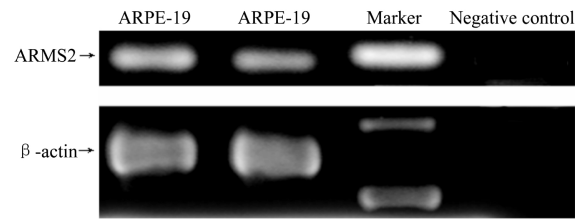

Figure 1 RT-PCR analysis of ARMS2 expression in ARPE-19 cells Agarose gel electrophoresis of PCR products amplified with ARMS2- (upper) and β-actin- (lower) specific primers. cDNA came from ARPE-19 cells (lane 1, 2). Lane 4 shows the negative control, substituting water for the cDNA template. Arrows to the right identify the expected size of the PCR DNA for ARMS2 (246 bp) and for β-actin (856 bp).

a concentration of 10^7/mL (we called it "LBs medium") at 37℃ for 10 minutes. Subsequently, each well of subconfluent cells was layered with 2 mL of LBs medium and was incubated at 37℃. After 12, 18, or 24 hours of incubation, the cells were washed 3 times with PBS to remove unbound LBs, detached using 0.05% trypsin/0.02% EDTA, washed twice with PBS, and then resuspended in 0.2mL of PBS for the flow cytometric assay (BD FACSCalibur; Becton Dickinson, San Jose, CA, USA). During the procedure for flow cytometric assay, the cells were analyzed with 488-nm excitation and a 530 ±15nm band-pass filter in the emission path. A negative control, consisting of untreated cells, was used to set the gate in each experiment. Each fiow cytometry run consisted of 10000 scattering events. To facilitate observation, some cultures were fixed at the end of the LBs challenge with 2% paraformaldehyde in 0.1mol/L phosphate buffer, pH 7.4, for 15 minutes at room temperature for subsequent imaging by confocal laser scanning fiuorescence microscopy (Nikon/C1 Plus; Nikon, Tokyo, Japan).

Statistical Analysis All experiments were performed at least in triplicate, and the mean and SD of the mean (mean± SD) were calculated. The statistically significant differences between the two samples were identified with SPSS 10.0, using Student's t-test; $P<0.05$ was considered significant.

RESULTS

Expression of ARMS2 in ARPE-19 Cells We used Reverse transcriptase PCR (RT-PCR) and immunofluorescence to test whether ARMS2 was expressed in ARPE-19 cells. RT-PCR analysis, using the full-length primers of ARMS2, confirmed that ARMS2 mRNA was expressed in ARPE-19 cells (Figure 1). The two bands of 246 bp and 856 bp presented the product from amplification with ARMS2-specific primers and β-actin-specific primers, respectively. Both products were of the expected size, based on the respective primer sets. Immunocytochemical analyses using anti-ARMS2 antibodies showed that ARMS2 was localized in the cytosol of the perinuclear region in
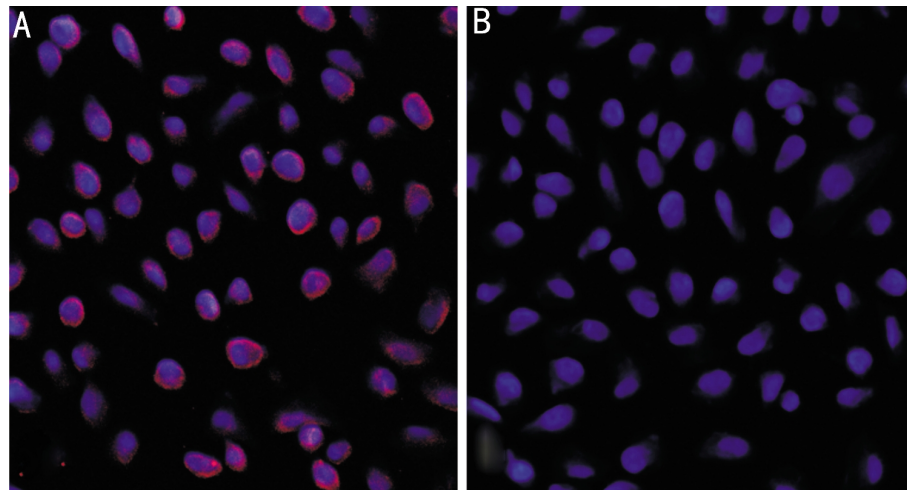
Figure 2 Immunocytochemistry staining of ARMS2 in ARPE−19 cells A: Immunocytochemistry staining of ARMS2 in ARPE-19 cells using ARMS2 primary antibody shows ARMS2 is mainly localized in the perinuclear region; B: In the absence of primary antibody, no staining was observed. Counterstaining with DAPI nuclear dye (blue). The original magnification was 400X.
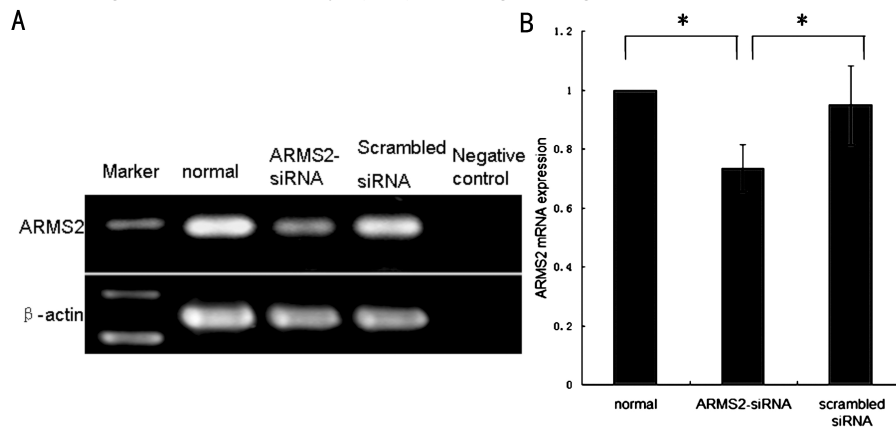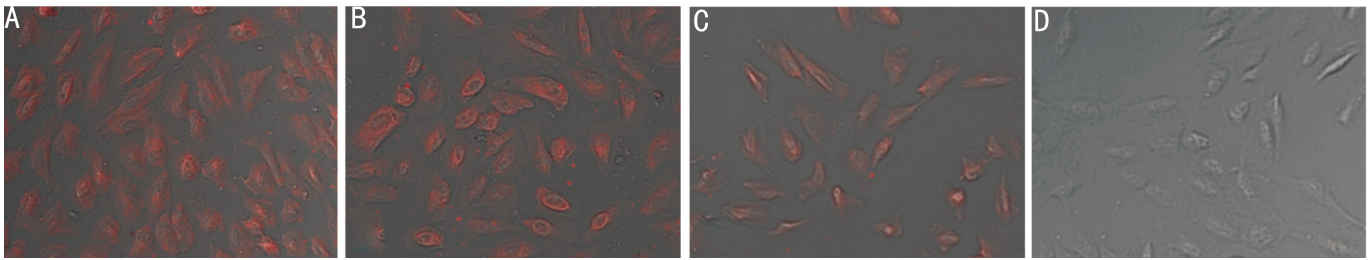

Figure 3 siRNA reduces the mRNA level of ARMS2 A: RNA was extracted from normal cells (lane 2) or cells treated with ARMS2-siRNA (lane 3) and scrambled siRNA (lane 4) for 24 hours at 25 nmol/L concentration. Following reverse transcription to cDNA, the samples were analyzed by RT-PCR using ARMS2- (upper) and β-actin- (lower) specific primers. Lane 5 shows the negative control, substituting water for the cDNA template; B: The bar graph shows the mean expression levels of ARMS2 transcript normalized to β-actin relative to that of the normal control. The asterisk indicates that the ARMS2-siRNA groups are significantly different from the normal groups and the scrambled siRNA groups (Student's t test, n =4, $*P$<0.05).

ARPE-19 cells (Figure 2). Experiments using normal nonimmune serum confirmed the specificity of this immunostaining. Furthermore, in multiple separated experiments, this pattern of staining held constant.

Suppression of ARMS2 Expression by siRNA in ARPE−19 cells We transfected ARPE-19 cells with one siRNA designed from the human ARMS2 gene sequence, and we measured the inhibitory effect of ARMS2 siRNA using RT-PCR and immunofluorescence methods. The mRNA level of ARMS2 was analyzed by RT-PCR, in which ARMS2 mRNA was co-amplified with β-actin mRNA in the same reaction. As shown in Figure 3A, except for the negative control group, all PCR products showed a specific band at the predicted sizes of 246 bp for ARMS2 and 856 bp for β-actin. The relative ratios of ARMS2 and β-actin PCR product quantities were determined by densitometric analysis. The results (1.00, 0.95 and 0.73,

respectively) were expressed as a percentage of the normal group, normalized to the corresponding co-amplified β-actin mRNA level. In the normal group (1.00 ±0.00) and the scrambled siRNA-transfected group (0.95±0.13), ARMS2 mRNA expression was similar, and no significant differences were found in these two groups (P=0.468), while in the ARMS2-siRNA-transfected group (0.73±0.08), siRNA induced a marked decrease in signal intensity for ARMS2, compared to the other two groups (P values were 0.001 and 0.033, respectively.). Densitometric analysis showed a 27% reduction of ARMS2 expression in the ARMS2-siRNA-treated samples (Figure 3B). Immunofluorescence showed evident staining of ARMS2 in the cytoplasm of untransfected cells (Figure 4A). Cells treated with scrambled siRNA (Figure 4B) exhibited a similar staining intensity as the untransfected cells. In the case of ARMS2-siRNA-transfected cells, we observed that ARMS2

Figure 4 siRNA reduces the protein level of ARMS2 Immunocytochemistry staining indicated the expression of ARMS2 decreased in ARPE-19 cells transfected with ARMS2-siRNA (C) when compared with cells transfected with scrambled siRNA (B) or without transfection (A). Negative control experiments were performed by omitting the primary antibody (D). The original magnification was 400X.
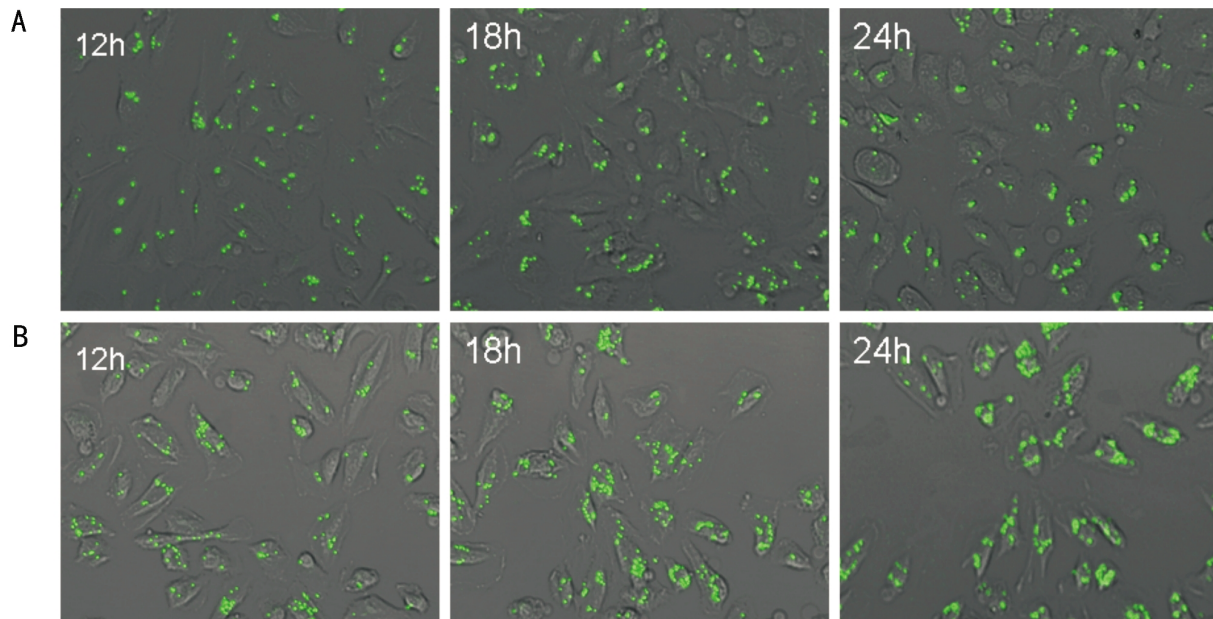
Figure 5 Phagocytosis of fluorescent-labeled latex beads (LBs) by ARMS2-siRNA or scrambled siRNA transfected ARPE-19 cells The cells were pre-treated with ARMS2-siRNA (A) or scrambled siRNA (B), then challenged with LBs for 12, 18, and 24 hours. The quantity of the LBs phagocytosed by ARPE-19 cells was increased, along with the extension of the time that the cells were incubated with LBs in all groups. Transfection with ARMS2-siRNA resulted in a drastic decrease in phagocytosis, compared with transfection with scrambled siRNA at all time points. The original magnification was 400X.

labeling was very faint (Figure 4C). No staining was observed in negative control cells, which omitted the primary antibody (Figure 4D). All the results indicated that ARMS2-siRNA efficiently silenced ARMS2 expression in ARPE-19 cells.

Quantification of Phagocytosis Functionally, RPE cells are among the most active phagocytic cells in the body. We performed in vitro phagocytosis assays that quantified the uptake of fluorescent-labeled latex beads (LBs) by ARPE-19, to determine whether ARMS2 may play a role in RPE phagocytosis. To determine the relevance of ARMS2 in RPE cell phagocytosis more directly, we used an RNA interference method to knock down ARMS2 expression. Confocal laser scanning fiuorescence microscopy examination confirmed that all beads identified in association with the cells were internalized and present within the cytoplasm. It also showed that transfection with ARMS2-siRNA (Figure 5A) significantly reduced ARPE-19

phagocytosis of LBs, compared to scrambled siRNA treatment (Figure 5B). We compared the effects of silencing ARMS2 expression from ARPE-19 cells on LBs phagocytosis using flow cytometric assay. Transient transfections with ARMS2-siRNA (Figure 6A) resulted in a drastic decrease in phagocytosis, compared with transfection with scrambled siRNA (Figure 6B) at all time points (Figure 6C and Table 1).

DISCUSSION

AMD, a degenerative disorder of the central retina and a major cause of legal blindness in industrialized countries [1], is broadly classified as either dry (atrophic) or wet (exudative) [23]. The dry form, which results in slowly progressive central visual loss, is characterized by drusen formation on the macula, degeneration of the RPE, and photoreceptor death [24]. The more severe wet form is characterized by choroidal neovascularization (CNV), leading to edema beneath the macula and rapidly
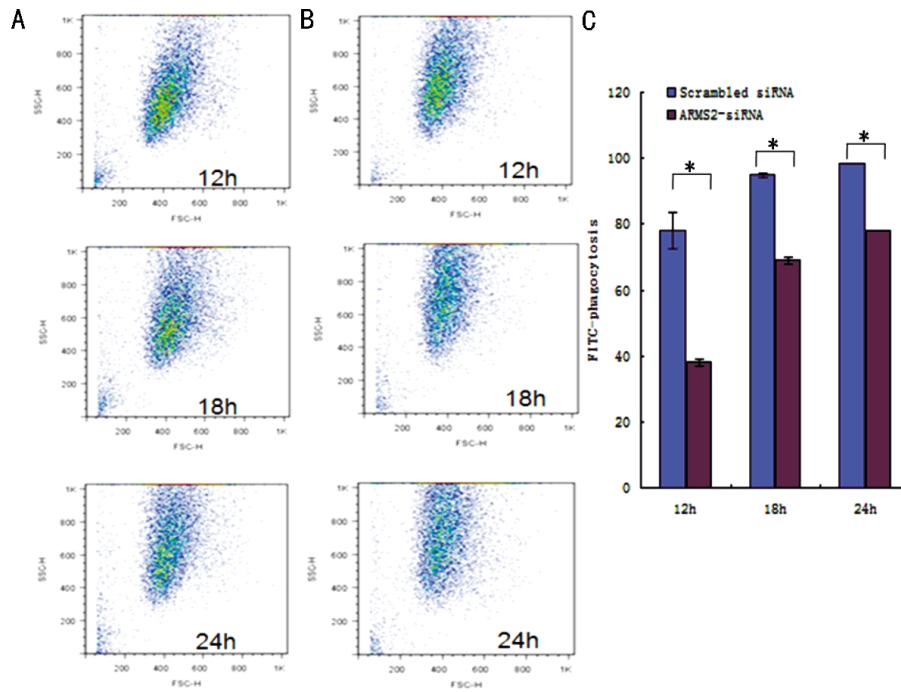
Figure 6 Quantification of phagocytosed fluorescent–labeled latex beads (LBs) using flow cytometric assay A: Flow cytometry analysis results for the ARMS2-siRNA-transfected cells' phagocytosis of LBs at 12, 18, and 24 hours; B: Flow cytometry analysis results for the scrambled siRNA-transfected cells' phagocytosis of LBs at 12, 18, and 24 hours; C: The data obtained by fiow cytometry are expressed as a histogram; ARMS2-siRNA significantly reduced ARPE-19's phagocytosis of LBs, compared to scrambled siRNA treatment (Student's t-test, n =3, * P <0.001).

Table 1 The quantification of the phagocytosis of siRNA-transfected ARPE-19 cells at different times

Group	n	12h	18h	24h
Scrambled siRNA	3	77.98±5.43	94.87±0.60	98.30±0.11
ARMS2-siRNA	3	38.04±1.02*	68.92±0.92*	78.00±0.12*

Student's t-test was used for comparison of phagocytosis of fluorescent-labeled Latex beads (LBs) by ARMS2-siRNA and scrambled siRNA transfected ARPE-19 cells at different times, which revealed a significant decrease of phagocytosis after 24-h ARMS2-siRNA treatment, * P <0.01.

progressive central visual loss [25]. Patients with dry AMD have a substantial risk of developing wet AMD.

The pathogenesis of the disease is also poorly understood, although several lines of evidence have indicated that dysfunction of the RPE is a crucial event in the molecular pathogenesis of AMD [26]. The RPE, a monolayer of polarized epithelial cells at the interface of the photoreceptor layer and Bruch's membrane, forms the outermost layer of the retina and performs multiple tasks that are of vital importance for the long-term preservation of retinal integrity and visual function. Critical roles for the RPE include phagocytic uptake and degradation of the constantly shed photoreceptor outer segments (POS), maintenance of the visual cycle by uptake, processing, transport and release of vitamin A, formation of the outer blood-retinal barrier and so on [26].

Twin studies and segregation analyses have determined that heredity is the primary contributor to the susceptibility of patients to developing AMD [3,4]. ARMS2 is the second major susceptibility gene for AMD, contributing independently of CFH to disease risk [6]. Kanda *et al*[13]

demonstrated that ARMS2 was expressed in the human retina and in a variety of other tissues and cell lines and that it encoded a 12-kDa protein, which localizes to the mitochondrial outer membrane when expressed in mammalian cells. They further reported that ARMS2 is localized to the ellipsoid region of the photoreceptors in the retina, where most of the mitochondria are located. Fritsche *et al* [16] demonstrated this finding and showed a minor dot-like staining in the ellipsoid region of the rod and cone inner segments, which fully co-localize with mitochondrial markers. However, Wang *et al* [27] indicated that ARMS2 was distributed in the cytosol and not in the mitochondrial outer membrane.

In the present study, we showed that ARMS2 is expressed in ARPE-19 cells. We found that ARMS2 was localized in the cytosol of the perinuclear region in ARPE-19, by immunocytochemical analyses using anti-ARMS2 antibodies. In our preliminary experiment, we found that ARMS2 protein was expressed on the apical surface of RPE cells. The staining on the apical surface, which has a large number of microvilli, is more prominent compared to other

regions (data not shown). The long apical microvilli are directly bound up with RPE phagocytosis [28]. In the mammalian retina, each RPE cell underlies -30 photoreceptor neurons. Every morning, stimulated by light and by circadian rhythms, stacks of POS membranes are shed from the distal ends of the photoreceptors[29]. Then, the long apical microvilli of the differentiated RPE cells ensheathe the POS, efficiently phagocytosing them [30]. Failure of this function has been implicated in some key pathological pathways of AMD, including lipofuscin accumulation [31,32] and drusen formation [33,34], eventually resulting in irreversible degeneration of the photoreceptor cells and loss of central vision[35,36].

The phagocytosis of POS is one of the most important functions of the RPE. This process is receptor-mediated[37], but the receptors and ligands involved in the phagocytosis of RPE cells are still unclear. To date, only a few RPE plasma membrane receptor proteins have been described as being involved in phagocytosis, such as mannose receptor protein[38], the lipid scavenger receptor protein CD36 [39], and the integrin αvβ5 [40,41]. All of these proteins can be detected in the microvilli. Now, we demonstrated a highly abundant expression of ARMS2 in the microvilli, and we supposed that ARMS2 might also participate in RPE phagocytosis. Moreover, Wang *et al* [27] found that ARMS2 containing the A69S replacement seems to be co-localized and distributed along the cytoplasmic skeleton, including the microtubules and actin, and not in any other cellular organelles in transfected COS7 cells. Due to the cytoplasmic skeleton involved in RPE phagocytosis [42,43], based on the information above and our finding, we had reason to believe that ARMS2 may also participate in RPE phagocytosis. To address this question, we investigated a potential role for this protein in RPE phagocytosis.

Philp *et al* [44] showed that RPE cells can phagocytose latex beads *in vitro*. Therefore, we selected fluorescent latex beads for the analysis of phagocytosis. siRNA technology was used to knock down the expression of ARMS2 in ARPE-19 cells. We measured the inhibitory effect of ARMS2 siRNA using RT-PCR and immunofluorescence, both of which showed effective silencing of ARMS2 expression by siRNA in cells. From the figure captured by confocal microscopy, we can see that the beads were internalized and present within the cytoplasm of ARMS2-siRNA- and scrambled siRNA-transfected cells, and the number of the beads increased with the extension of the duration of incubation with LBs. It was also obvious that transfection with ARMS2-siRNA resulted in a drastic decrease in phagocytosis, compared with transfection with scrambled siRNA at all time points. This result was con rmed more objectively by flow cytometric assay. Thus, we demonstrated that ARMS2 plays a part in the phagocytosis of LBs by ARPE-19 cells.

In conclusion, our results suggested that there was endogenous expression of ARMS2, both in ARPE-19 cells and in human retina tissue. In ARPE-19, ARMS2 was localized in the cytosol of the perinuclear region. In human retina tissue, ARMS2 was enriched on the apical surface, which has a large number of microvilli. More importantly, our data indicated that ARMS2 may play a role in phagocytosis of the RPE, and this may be one of the mechanisms that participates in the development of AMD. However, the exact mechanism requires further investigation.

REFERENCES

1 Friedman DS, O'Colmain BJ, Munoz B, Tomany SC, McCarty C, de Jong PT, Nemesure B, Mitchell P, Kempen J. Prevalence of age-related macular degeneration in the United States. *Arch Ophthalmol* 2004; 122: 564-572

2 Gorin MB, Breitner JC, de Jong PT, Hageman GS, Klaver CC, Kuehn MH, Seddon JM. The genetics of age-related macular degeneration. *Mol Vis* 1999; 5:29

3 Swaroop A, Branham KE, Chen W, Abecasis G. Genetic susceptibility to age-related macular degeneration: a paradigm for dissecting complex disease traits. *Hum Mol Genet* 2007; 16:R174-182

4 Gorin MB. A clinician's view of the molecular genetics of age-related maculopathy. *Arch Ophthalmol* 2007;125:21-29

5 Klein RJ, Zeiss C, Chew EY, Tsai JY, Sackler RS, Haynes C, Henning AK, SanGiovanni JP, Mane SM, Mayne ST, Bracken MB, Ferris FL, Ott J, Barnstable C, Hoh J. Complement factor H polymorphism in age-related macular degeneration. *Science* 2005;308:385-389

6 Rivera A, Fisher SA, Fritsche LG, Keilhauer CN, Lichtner P, Meitinger T, Weber BH. Hypothetical LOC387715 is a second major susceptibility gene for age-related macular degeneration, contributing independently of complement factor H to disease risk. *Hum Mol Genet* 2005;14:3227-3236

7 Edwards AO, Ritter RIII, Abel KJ, Manning A, Panhuysen C, Farrer LA. Complement factor H polymorphism and age-related macular degeneration. *Science* 2005; 308:421-424

8 Weeks DE, Conley YP, Mah TS, Paul TO, Morse L, NgoChang J, Daily JP, Ferrell RE, Gorin MB. A full genome scan for age-related maculopathy. *Hum Mol Genet* 2000; 9:1329-1349

9 Seddon JM, Santangelo SL, Book K, Chong S, Cote J. A genome wide scan for age-related macular degeneration provides evidence for linkage to several chromosomal regions. *Am J Hum Genet* 2003;73:780-790

10 Kenealy SJ, Schmidt S, Agarwal A, Postel EA, De La Paz MA, Pericak-Vance MA, Haines JL. Linkage analysis for age-related macular degeneration supports a gene on chromosome 10q26. *Mol Vis* 2004;10: 57-61

11 Fisher SA, Abecasis GR, Yashar BM, Zareparsi S, Swaroop A, Iyengar SK, Klein BE, Klein R, Lee KE, Majewski J, Schultz DW, Klein ML, Seddon JM, Santangelo SL, Weeks DE, Conley YP, Mah TS, Schmidt S, Haines JL, Pericak-Vance MA, Gorin MB, Schulz HL, Pardi F, Lewis CM, Weber BH. Meta-analysis of genome scans of age-related macular degeneration. *Hum Mol Genet* 2005;14:2257-2264

12 Jakobsdottir J, Conley YP, Weeks DE, Mah TS, Ferrell RE, Gorin MB. Susceptibility genes for age-related maculopathy on chromosome 10q26. *Am J Hum Genet* 2005; 77:389-407

13 Kanda A, Chen W, Othman M, Branham KE, Brooks M, Khanna R, He S, Lyons R, Abecasis GR, Swaroop A. A variant of mitochondrial protein LOC387715/ARMS2, not HTRA1, is strongly associated with age-related macular degeneration. *Proc Natl Acad Sci USA* 2007; 104:16227–16232

14 Ross RJ, Bojanowski CM, Wang JJ, Chew EY, Rochtchina E, Ferris FL 3rd, Mitchell P, Chan CC, Tuo J. The LOC387715 polymorphism and age-related macular degeneration: replication in three case-control samples. *Invest Ophthalmol Vis Sci* 2007; 48:1128–1132

15 Tong Y, Liao J, Zhang Y, Zhou J, Zhang H, Mao M. LOC387715/HTRA1 gene polymorphisms and susceptibility to age-related macular degeneration: A HuGE review and meta-analysis. *Mol Vis* 2010;16: 1958–1981

16 Fritsche LG, Loenhardt T, Janssen A, Fisher SA, Rivera A, Keilhauer CN, Weber BH. Age-related macular degeneration is associated with an unstable ARMS2 (LOC387715) mRNA. *Nat Genet* 2008; 40:892–896

17 Gotoh N, Nakanishi H, Hayashi H, Yamada R, Otani A, Tsujikawa A, Yamashiro K, Tamura H, Saito M, Saito K, Iida T, Matsuda F, Yoshimura N. ARMS2 (LOC387715) variants in Japanese patients with exudative age-related macular degeneration and polypoidal choroidal vasculopathy. *Am J Ophthalmol* 2009; 147(6):1037? 041, 1041.e1–2

18 Wang G, Spencer KL, Scott WK, Whitehead P, Court BL, Ayala-Haedo J, Mayo P, Schwartz SG, Kovach JL, Gallins P, Polk M, Agarwal A, Postel EA, Haines JL, Pericak-Vance MA. Analysis of the indel at the ARMS2 3'UTR in age-related macular degeneration. *Hum Genet* 2010; 127(5):595–602

19 Xu YL, Guan N, Xu J, Yang XF, Ma K, Zhou HY, Zhang F, Snellingen T, Jiao YQ, Liu XP, Wang NL, Liu NP. Association of CFH, LOC387715, and HTRA1 polymorphisms with exudative age-related macular degeneration in a northern Chinese population. *Mol Vis* 2008;14:1373–1381

20 Chen LJ, Liu DT, Tam PO, Chan WM, Liu K, Chong KK, Lam DS, Pang CP. Association of complement factor H polymorphisms with exudative age-related macular degeneration. *Mol Vis* 2006;12:1536–1542

21 Gotoh N, Yamada R, Hiratani H, Renault V, Kuroiwa S, Monet M, Toyoda S, Chida S, Mandai M, Otani A, Yoshimura N, Matsuda F. No association between complement factor H gene polymorphism and exudative age-related macular degeneration in Japanese. *Hum Genet* 2006; 120:139–143

22 Fuse N, Miyazawa A, Mengkegale M, Yoshida M, Wakusawa R, Abe T, Tamai M. Polymorphisms in Complement Factor H and Hemicentin-1 genes in a Japanese population with dry-type age-related macular degeneration. *Am J Ophthalmol* 2006; 142:1074–1076

23 Dewan A, Liu M, Hartman S, Zhang SS, Liu DT, Zhao C, Tam PO, Chan WM, Lam DS, Snyder M, Barnstable C, Pang CP, Hoh J. HTRA1 promoter polymorphism in wet age-related macular degeneration. *Science* 2006; 314:989–992

24 Young RW (1987) Pathophysiology of age-related macular degeneration. *Surv Ophthalmol* 31:291–306

25 Green WR, Enger C. Age-related macular degeneration histopathologic studies. The 1992 Lorenz E. Zimmerman Lecture. *Ophthalmology* 1993; 100:1519–1535

26 Kaemmerer E, Schutt F, Krohne TU, Holz FG, Kopitz J. Effects of lipid peroxidation-Related Protein Modification on RPE Lysosomal Functions and POS Phagocytosis in human retinal pigment epithelial cells. *Invest Ophthalmol Vis Sci* 2007; 48:1342–1347

27 Wang G, Spencer KL, Court BL, Olson LM, Scott WK, Haines JL, Pericak-Vance MA. Localization of age-related macular degeneration-associated ARMS2 in cytosol, not mitochondria. *Invest Ophthalmol Vis Sci* 2009; 50:3084–3090

28 Spitznas M, Hogan MJ. Outer segments of photoreceptors and the retinal pigment epithelium. Interrelationship in human eye. *Arch Ophthalmol* 1970; 84:810–819

29 Young RW. The renewal of photoreceptor cell outer segments. *J Cell Biol* 1967; 33:61–72

30 Besharse JC, Defoe DM. Role of the retinal pigment epithelium in photoreceptor membrane turnover. In: Marmor MF, Wolfensberger TJ (eds) *The Retinal Pigment Epithelium* 1998; Oxford, UK, pp152–172

31 Kopitz J, Holz FG, Kaemmerer E, Schutt F. Lipids and lipid peroxidation products in the pathogenesis of age-related macular degeneration. *Biochimie* 2004;86:825–831

32 Sparrow JR, Boulton M. RPE lipofuscin and its role in retinal pathobiology. *Exp Eye Res* 2005; 80:595–606

33 Abdelsalam A, Del Priore L, Zarbin MA. Drusen in age-related macular degeneration: pathogenesis, natural course, and laser photocoagulation-induced regression. *Surv Ophthalmol* 1999; 44:1–29

34 Hageman GS, Luthert PJ, Victor Chong NH, Johnson LV, Anderson DH, Mullins RF. An integrated hypothesis that considers drusen as biomarkers of immune-mediated processes at the RPE–Bruch'smembrane interface in aging and age-related macular degeneration. *Prog Retin Eye Res* 2001; 20:705–732

35 Dowling JE, Sidman RL. Inherited retinal dystrophy in the rat. *J Cell Biol* 1962; 14:73–109

36 Bok D, Hall MO. The role of the pigment epithelium in the etiology of inherited retinal dystrophy in the rat. *J Cell Biol* 1971; 49:664–682

37 Young RW, Bok D. Participation of the retinal pigment epithelium in the rod outer segment renewal process. *J Cell Biol* 1969; 42:392–403

38 Boyle D, Tien LF, Cooper NG, Shepherd V, McLaughlin BJ. A mannose receptor is involved in retinal phagocytosis. *Invest Ophthalmol Vis Sci* 1991;32(5):1464–1470

39 Ryeom SW, Sparrow JR, Silverstein RL. CD36 participates in the phagocytosis of rod outer segments by retinal pigment epithelium. *J Cell Sci* 1996;109:387–395

40 Miceli MV, Newsome DA, Tate DJ Jr. Vitronectin is responsible for serum-stimulated uptake of rod outer segments by cultured retinal pigment epithelial cells. *Invest Ophthalmol Vis Sci* 1997; 38:1588–1597

41 Finnemann SC, Bonilha VL, Marmorstein AD, Rodriguez-Boulan E. Phagocytosis of rod outer segments by retinal pigment epithelial cells requires alpha(v)beta5 integrin for binding but not for internalization. *Proc Natl Acad Sci USA* 1997; 94:12932–12937

42 Finnemann SC, Rodriguez-Boulan E. Macrophage and Retinal Pigment Epithelium Phagocytosis: apoptotic cells and photoreceptors compete for avb3 and avb5 integrins, and protein kinase C regulates avb5 binding and cytoskeletal linkage. *J Exp Med* 1990; 190:861–874

43 Allen LA, Aderem A. Molecular definition of distinct cytoskeletal structures involved in complement- and Fc receptor-mediated phagocytosis in macrophages. *J Exp Med* 1996;184:627–637

44 Philp NJ, Bernstein MH. Phagocytosis by retinal pigment epithelium explants in culture. *Exp Eye Res* 1981; 33:47–53